Atomistic simulation of charged iron oxyhydroxide surfaces in contact with aqueous solution†

Sebastien Kerisit, David J. Cooke, Arnaud Marmier and Stephen C. Parker*

Received (in Cambridge, UK) 17th March 2005, Accepted 20th April 2005
First published as an Advance Article on the web 13th May 2005
DOI: 10.1039/b503899e

Molecular dynamics simulations of aqueous solution/goethite interfaces show that the classical models of the electrical double layer do not accurately describe the distribution of ions near the surface (such a distribution is present even when the surface is neutral) and that the explicit treatment of solvent molecules is essential to capture the effects of the surface on the liquid phase.

Heavy metal pollution of soils/sediments has increased significantly. The risks (toxicity, bioaccumulation) caused by this contamination need to be assessed and predicted. One of the key steps which controls their mobility and availability concerns their adsorption from solution onto mineral surfaces.[1] Iron hydroxides have an excellent capacity to accumulate metal pollutants by adsorption,[2] and are therefore prime candidates for reducing heavy metal mobility. The FeOOH family (α, goethite; β, akaganeite; γ, lepidocrocite) has received much attention and been the subject of many experimental studies (for example ref. 3–5). Surface Complexation Models (SCM), which have been used to study the adsorption of heavy metals under different conditions (concentration, pH, ionic strength), are known to depend significantly on the chemical and physical representation of the surface.[6–8] There have only been a few atomistic modelling studies of this type of system. For example, one used GGA-DFT[9] with localised orbitals, and a small cluster, but did not include water. The surface of goethite and its interaction with impurities has also been partially treated with atomistic models and energy optimisation strategies,[10,11] but again without explicit, dynamical treatment of the water. A third way is desirable, where there is a discrete description of all of the constituent species, including water, ions, atoms, and at a scale big enough to provide a realistic treatment of the surfaces and their environment. This would provide a reliable set of structural data for SCMs and enable one to ascertain directly the mode of adsorption of heavy metals on goethite, whether inner sphere, outer sphere or surface precipitation, as a function of surface charge. Thus, the aim of this study is to establish the viability of atomistic simulations for modelling ionic distributions and coordinations as a function of distance to neutral and charged mineral surfaces.

Molecular dynamics (MD) simulations of a (100) goethite slab in contact with pure and salted water were performed using the computer code DL_POLY.[12] These calculations are based on the Born model of solids,[13] in which the atoms of a system interact *via* long-range electrostatic forces and short-range interactions. The latter are described by parametrised functions and represent the repulsion between electron charge clouds, the van der Waals attraction forces, and, where appropriate, many body terms such as bond bending. In addition, the polarisability of anions was accounted for by the shell model of Dick and Overhauser,[14] whereby the polarisable ions consist of two particles, a core and a shell, coupled by a harmonic spring. The potential parameters for the intra- and intermolecular interactions of water are those derived by de Leeuw and Parker[15] with the revised hydrogen bond parameters of Kerisit and Parker.[16] The goethite mineral and its interactions with water were modelled using potential parameters based on the work of Lewis and Catlow[17] together with the Baram and Parker[18] model of the hydroxyl ion. The chloride–water potential was developed for this study to reproduce the structure and energetics of small halide–water clusters obtained from *ab initio* calculations and the sodium–water potential was derived by Post and Burnham.[19] The sodium chloride model is that of Catlow *et al.*[20] The potential set is collected into a table and presented as supplementary data.† The mineral slab, which contained 192 FeOOH units, had a thickness of 16 Å and a surface area of 18.80 × 18.87 Å^2. The mineral slab was put in contact with two slabs of water of a thickness ranging from 35 Å to 180 Å and containing between 480 and 2880 water molecules each. A vacuum of 100 Å was introduced between the two water slabs. In the simulations containing dissolved salt, between 8 and 48 sodium and chloride ions were introduced in each water slab. All the simulations where performed in the NVT ensemble (*i.e.*, constant number of particles, constant volume, and constant temperature) at 300 K and zero applied pressure up to 1.5 ns. The temperature was kept constant by use of the Nosé–Hoover thermostat.[21] The smooth particle mesh Ewald method (SPME)[22,23] was used to calculate the electrostatic interactions with a real space cutoff of 8 Å. The same cutoff was used for the short-range interactions. The particles' trajectories were generated by the Verlet Leapfrog algorithm with a time step of 0.2 fs. The shells were given a small mass of 0.2 a.u. following the approach introduced by Mitchell and Fincham.[24]

A slab of simulated goethite crystal was cut exposing (100) surfaces, which are comprised of alternating layers containing either hydroxide groups or iron and oxygen atoms. There are, therefore, two possible terminations and according to our static calculations, the most stable surface is that terminated by a hydroxide layer, as shown in Fig. 1. The surface hydroxyl ions are bonded to two cations from the Fe–O layer below. In this layer, the iron atoms are in five-fold coordination, whereas the oxygen ions remain in their bulk coordination and are bonded to three cations. In vacuum, the hydroxyl ions rotate to point away from the surface and the surface is thus

† Electronic supplementary information (ESI) available: Potential set. See http://www.rsc.org/suppdata/cc/b5/b503899e/

*s.c.parker@bath.ac.uk

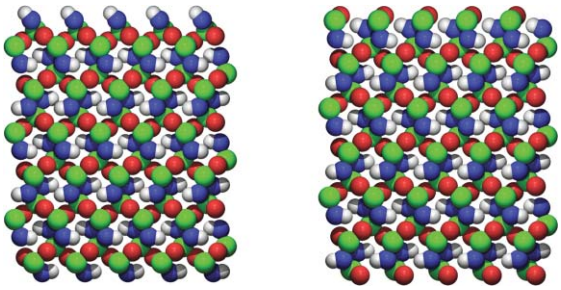

Fig. 1 Side view of the two possible surface terminations of the (100) surface of goethite, where iron, oxygen, hydroxyl oxygen and hydrogen are coloured green, red, blue and white respectively.

corrugated with grooves in between hydroxyl rows that are 4.7 Å wide.

Next, we immersed the slab of mineral in water and performed a MD simulation, monitoring the atoms' trajectory over 1 ns. The analysis of the water density as a function of distance in the direction normal to the surface reveals a clear layering up to 15 Å from the surface (see Fig. 2), where the surface is defined as the plane passing through the centre of the uppermost layer of iron atoms. Similar behaviour has been observed in the vicinity of other mineral surfaces both in experimental[25–27] and theoretical studies.[16,28,29] The first peak corresponds to water molecules adsorbed in the surface's grooves at a height of 1.8 Å above the surface. The second peak corresponds to those molecules that are bonded to surface hydroxyls. Each layer contained on average one water molecule per surface cation and thus the period of oscillation is similar to the size of a water molecule, *i.e.* 1.5 Å. The calculation of water residence times shows that water molecules in the first layer remain adsorbed in the surface's groove for half a nanosecond. Fig. 2 also shows small oscillations of the water density at the liquid–vapour interface.

We then introduced sodium and chloride ions randomly into the water layers, excluding the first two layers adjacent to the mineral surface, so that the salt concentration was 1.2 mol dm^{-3}, *i.e.*, about twice that in sea water. Two different starting configurations were generated and the sodium, chloride, and water distributions were calculated from the average of the two simulations. Although the presence of electrolyte ions causes local disruptions of the water hydrogen bond structure, the shape of the water density profile is unaffected by the presence of electrolyte ions. Fig. 2 shows the sodium and chloride distributions in the direction normal to the surface. There are two main points to note from this figure. Firstly, both the sodium and chloride distributions show layering in the region closest to the surface. The oscillations persist to about 12 Å and their period reproduces that of water, although this is more obvious for chloride than for sodium. Secondly, there is a clear build up of negative charge near the surface due to the adsorption of chloride ions in the third and fourth hydration layers and the fact that this region is depleted in sodium ions. However, beyond about 8 Å, the chloride concentration decreases sharply and there is a large excess of sodium ions in the next 10 Å. The positive charges accumulate to compensate for the excess of chloride ions in the first few hydration layers. In turn, this excess of sodium ions is itself compensated by a build up of chloride ions in the following 10 Å. The result is that there are oscillations of the overall salt charge distribution, as shown in Fig. 3. This calculated distribution differs significantly in shape from the classical view of the electrical double layer in the vicinity of a mineral surface, whereby, beyond the Stern layer, the net electrical charge is thought to decay exponentially. Further evidence that the oscillations in net charge densities may be common include recent molecular dynamics simulations of molten and gaseous sodium chloride by Keblinski *et al.*,[30] who showed that what they call "strongly-coupled regimes", developed such oscillations. These results in turn are similar to calculations at very high salt concentrations by Spohr.[31] As the original models of the ionic distributions in the double layer were derived from a consideration of the electrostatic potential we investigated how the potential is modified by the calculated interface.

The electrostatic potential in the direction normal to the surface was calculated by solving the one dimensional Poisson equation for the simulations containing both pure water and salt solution. The electrostatic potential was found to be very similar in both cases as shown in Fig. 3. Due to the specific orientation of water molecules near the surface, the electrostatic potential shows narrow peaks up to 6 Å. Beyond this height, the peaks become very broad and their amplitude is slightly affected by the presence of electrolyte ions. In this region, there is a striking correlation with the salt charge distribution, which would imply that the modification of the water structure caused by the mineral surface controls the distribution of electrolyte ions in the vicinity of this charge-neutral surface.

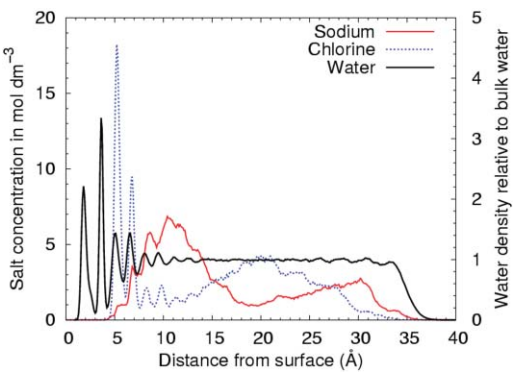

Fig. 2 The variation of salt concentration as a function of distance from the goethite surface in comparison to the water density.

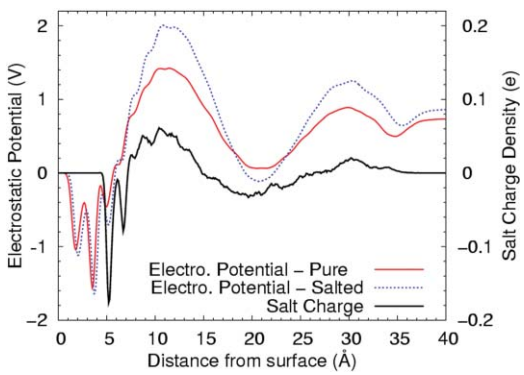

Fig. 3 The variation of electrostatic potential as a function of distance from the goethite surface in comparison to the salt charge density.

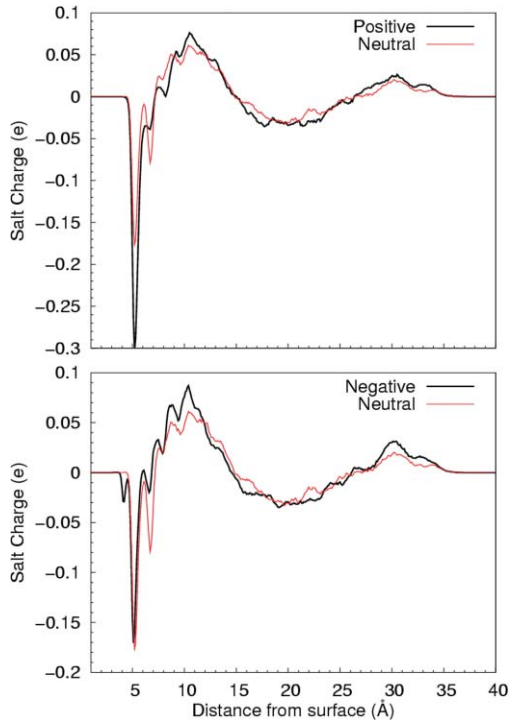

Fig. 4 Comparison of the net charge distribution in solution in contact with a neutral and positively charged surface.

As the charge on a mineral surface is another significant parameter two simulations were performed to investigate the effect of the surface charge on the distribution of electrolyte ions. In the first simulation, a hydroxyl group was removed from each surface of the slab to form positively charged surfaces and the system was neutralised by adding a chloride ion in each water slab. In the second simulation, a hydroxyl group from each surface was replaced by an oxygen atom to create negatively charged surfaces and the system was charge compensated by adding a sodium ion in each water slab. The charges at the positive and negative surfaces were 4.5 and -4.5 μC cm^{-2}, respectively. The negatively charged surface still shows the same chloride peak near the surface but also a slight increase in sodium density near the interface (see Fig. 4). On the positively charged surface, the distribution is identical to that of the neutral surface except for a larger first chloride peak. However, in both cases these changes are small and the overall shape of the salt distribution is unaffected.

We also performed molecular dynamics simulations of sodium chloride solutions in contact with two different mineral surfaces, namely, the {10.4} calcite surface ($CaCO_3$) and the {01.2} hematite surface (Fe_2O_3). These calculations showed the same principal features, *i.e.*, the oscillatory behaviour of the charge distribution and the clear correlation with the electrostatic potential in the aqueous solution. These results suggest that the occurrence of such features is not strongly dependent on the nature of the mineral surface.

To conclude, these calculation suggest that the classical models are correct in assuming that the ion distribution is controlled by the electrostatic potential. They nevertheless fail to reproduce the distribution at high salt concentration because they neglect the electrostatic contribution of the solvent. This is further reinforced by the fact that the effect of surface charge, at the level considered here, is limited.

Thus, the explicit treatment of solvent molecules is crucial to capture all the effects of the mineral surface on the liquid phase. This communication highlights that atomistic simulations can be used to reconsider and extend phenomenological models in order to depict a more comprehensive picture of the solid–liquid interface.

We would like to acknowledge EPSRC for funding (grant GR/HO413), the NERC e-science initiative and the Materials Chemistry Consortium for the provision of computer time.

Sebastien Kerisit, David J. Cooke, Arnaud Marmier and Stephen C. Parker*
Department of Chemistry, University of Bath, Claverton Down, Bath, UK BA2 7AY. E-mail: s.c.parker@bath.ac.uk

Notes and references

1 A. M. Shiller and E. A. Boyle, *Geochim. Cosmochim. Acta*, 1987, **51**, 3273.
2 A. Tessier, D. Fortin, N. Belzile, R. R. DeVitre and G. G. Leppard, *Geochim. Cosmochim. Acta*, 1996, **60**, 387.
3 M. McBride, C. E. Martinez and S. Sauve, *Soil Sci. Soc. Am. J.*, 1998, **62**, 1542.
4 C. A. Christophi and L. Axe, *J. Environ. Eng.*, 2000, **126**, 66.
5 K. J. Wang and B. S. Xing, *Chemosphere*, 2002, **48**, 665.
6 J. Lutzenkirchen, *Aquat. Geochem.*, 2001, **7**, 217.
7 K. F. Hayes and J. O. Leckie, *J. Colloid Interface Sci.*, 1987, **115**, 564.
8 C. E. Cowan, J. M. Zachara and C. T. Resch, *Environ. Sci. Technol.*, 1991, **25**, 437.
9 S. R. Randall, D. M. Sherman, K. V. Ragnarsdottir and C. R. Collins, *Geochim. Cosmochim. Acta*, 1999, **63**, 2971.
10 A. R. Felmy and J. R. Rustad, *Geochim. Cosmochim. Acta*, 1998, **62**, 25.
11 H. M. Steele, K. Wright and I. H. Hillier, *Geochim. Cosmochim. Acta*, 2002, **66**, 1305.
12 W. Smith and T. R. Forester, DL_POLY is a package of molecular simulation routines written by W. Smith and T. R. Forester, copyright The Council for the Central Laboratory of the Research Councils, Daresbury Laboratory at Daresbury, Nr. Warrington, UK, 1996.
13 M. Born and K. Huang, *Dynamical Theory of Crystal Lattices*, Oxford University Press, Oxford, UK, 1954.
14 B. G. Dick and A. W. Overhauser, *Phys. Rev.*, 1958, **112**, 90.
15 N. H. de Leeuw and S. C. Parker, *Phys. Rev. B*, 1998, **58**, 13901.
16 S. Kerisit and S. C. Parker, *J. Am. Chem. Soc.*, 2004, **126**, 10152.
17 G. V. Lewis and C. R. A. Catlow, *J. Phys. C: Solid State Phys.*, 1985, **18**, 1149.
18 P. S. Baram and S. C. Parker, *Philos. Mag. B*, 1996, **73**, 49.
19 J. E. Post and C. W. Burnham, *Am. Mineral.*, 1986, **71**, 142.
20 C. R. A. Catlow, K. M. Diller and M. J. Norgett, *J. Phys. C: Solid State Phys.*, 1977, **10**, 1395.
21 W. G. Hoover, *Phys. Rev. A*, 1985, **31**, 1695.
22 P. P. Ewald, *Ann. Phys.*, 1921, **64**, 253.
23 U. Essmann, L. Perera, M. L. Berkowitz, T. Darden, H. Lee and L. G. Pedersen, *J. Chem. Phys.*, 1995, **103**, 8577.
24 P. J. Mitchell and D. Fincham, *J. Phys.: Condens. Matter*, 1993, **5**, 1031.
25 J. N. Israelachvili and R. M. Pashley, *Nature*, 1983, **306**, 249.
26 P. Fenter, L. Cheng, C. Park, H. Zhang and N. C. Sturchio, *Geochim. Cosmochim. Acta*, 2003, **67**, 4267.
27 L. Cheng, P. Fenter, K. L. Nagy, M. L. Schlegel and N. C. Sturchio, *Phys. Rev. Lett.*, 2001, **87**, 156103.
28 M. I. McCarthy, G. K. Schenter, C. A. Scamehorn and J. B. Nicholas, *J. Phys. Chem.*, 1996, **100**, 16989.
29 E. Spohr, *J. Phys. Chem.*, 1989, **93**, 6171.
30 P. Keblinski, J. Eggebrecht, D. Wolf and S. R. Phillpot, *J. Chem. Phys.*, 2000, **113**, 282.
31 E. Spohr, *J. Electroanal. Chem.*, 1998, **450**, 327.